

COMPARISON OF COMPLEX MODULUS DATA GENERATED BY THREE DIFFERENT MEASUREMENT TECHNIQUES

By

Michael L. Drake and Anil Sircar
University of Dayton Research Institute
Dayton, OH 45469
(513) 229-2644

INTRODUCTION

There are many different test instruments which can determine the complex modulus properties of materials, and there are numerous ways that these complex data can be displayed on a reduced frequency nomogram (RFN). This paper will present the complex modulus properties of Dyad 609 which is a commercially available copolymer marketed by the Soundcoat Company and a highly loaded UDRI formulation of Vinac B-100. Vinac B-100 is a polyvinyl acetate material marketed by Air Products.

The three complex modulus test instruments evaluated were the ASTM E-756 BEAM Test system, the Polymer Laboratories DMTA machine, and the Rheometrics RSA II. Table 1 presents the basic temperature and frequency ranges over which each of these test instruments operate and the specimens which are typically used.

There were three different forms of the shift factor (α_T) used to develop the complex modulus data display on a RFN. The equations used were:

(1) the WLF equation [1]

$$\log \alpha_T = \frac{C_1(T-T_0)}{C_2+T-T_0}$$

where $C_1 = 12$ and $C_2 = 525$

(2) an Arrhenius equation [2]

$$\log \alpha_T = \frac{T_A}{T} - \frac{T_A}{T_0}$$

and

(3) a quadratic in $\frac{1}{T}$ where [3]

$$\log \alpha_T = (a[\frac{1}{T} - \frac{1}{T_z}] + 2.303[\frac{2a}{T_z} - b]) \log \frac{T}{T_z} + \frac{b}{T_z} - \frac{a}{T_z^2} - S_{AZ})(T-T_z)$$

The complex modulus data obtained from each test and the effects of the various α_T equations are presented in the following paragraphs.

DYAD 609

The Dyad 609 RFN from the BEAM test is given in Figure 1. There are 51 complex data points plotted. The temperature range for the test was -5°F to 246°F and the frequency range was 260 Hz to 3400 Hz. A free layer test specimen was used to determine the glassy modulus data and a sandwich test specimen was used to determine the transition and rubbery modulus data. The WLF form of α_T was used to generate Figure 1 and the T_0 value was chosen to be 240°F .

Figure 2 displays the S2-73 committee suggested inverted U plot of material loss factor versus magnitude Young's modulus. The switch from the free layer to sandwich test specimen data occurs near 10^5 PSI. The inverted U plot indicates that there is some scatter in the BEAM data; however, overall the data appears to be acceptable.

The Dyad 609 DMTA results are given in Figure 3 (RFN) and Figure 4 (inverted U). There are 211 complex modulus data points which cover the temperature range of 79°F to 212°F and a frequency range of 0.3 Hz to 30 Hz. A bending test specimen was used for the DMTA test. The WLF α_T with a T_0 of 356°F was used to generate Figure 3. Figure 4 illustrates very little scatter in the DMTA data.

The RSA II test results are given in Figure 5 (RFN) and Figure 6 (inverted U). There are 112 complex data sets plotted. These data cover the temperature from -20°F to 110°F and a frequency from 0.1 Hz to 15 Hz. A bending specimen was used in the RSA II test. The WLF α_T with $T_0 = 356^{\circ}\text{F}$ was used to generate Figure 5. Figure 6 illustrates the value of the inverted U plot. In Figure 6 it is obvious that the data near and above a modulus of 10^4 PSI is inaccurate. This problem developed from the geometry of the bending specimen used. To collect accurate data into the transition region through the rubbery region, a different geometry of bending specimen and a shear specimen would be required.

The reduced frequency data for all three tests appears, if viewed individually, to be a reasonable representation of the material properties. Table 2 presents a comparison of the nomogram data presented in Figures 1, 3, and 5. This table illustrates the significant difference in the three data sets.

In the WLF α_T equation, the value of the constants C_1 and C_2 were derived from the comparison of a large number of high frequency damping property tests. This is probably the reason that the T_0 for the BEAM data is so different from the T_0 of the DMTA and RSA II.

The value of the maximum material loss factor compares well for the BEAM and DMTA tests, however, the temperature at which the peak occurs is different by 14°F at 100 Hz. The temperature difference leads to the large variation in the modulus at peak damping determined by each test. Generally, at temperatures below peak damping, the BEAM data indicated a high modulus while at temperature above peak damping, the BEAM data indicated a lower modulus.

Figure 7 presents all three complex modulus data sets on the inverted U plot. The RSA II and DMTA data match quite closely up to the point where the RSA II data becomes unstable. The BEAM test data demonstrates a shift to higher modulus values across the range.

Figure 8 presents all three data sets on a RFN with $T_0 = 240^\circ\text{F}$. This T_0 is obviously inappropriate for the DMTA and RSA II data. Figure 9 presents the same data with $T_0 = 356^\circ\text{F}$. The BEAM and DMTA loss factor data collapse to the same curve. However, the modulus trend illustrated in Table 2 has changed in that the BEAM data now exhibits a higher modulus value across the entire range. This change in data comparison led to the investigation of other α_T equations.

Figure 10 presents the Dyad 609 data sets on a reduced frequency plot where α_T is equation Number 2. The loss factor trend and the modulus trend is the same as seen with the high value of T_0 in the $WLF\alpha_T$ RFN (Figure 9).

The current S2-73 draft standard uses the α_T equation Number 3. The BEAM and DMTA data were characterized using the S2-73 procedure. The BEAM data RFN in S2-73 draft standard form is presented in Figure 11; while the DMTA data RFN is presented in Figure 12. Again, both data sets when viewed independently appear to be reasonable characterizations of the damping material.

Table 3 compares the S2-73 characterization of the BEAM and DMTA data sets. The S2-73 characterization is conservative on the value of peak damping when compared to the other two methods; however, the tendency of the BEAM data to have a slightly lower temperature of peak damping at a given frequency is consistent with the previous characterization methods. The discerning thing in Table 3 is the modulus trend illustrated. In Table 3 it can be seen that the beam characterization has a lower modulus value across the board than the DMTA characterization.

Table 4 summarizes the variation in the complex modulus data at the peak loss factor between the four different α_T equations evaluated. The data in Table 4 combined with the data presented earlier in Figure 7 do make definite statements.

First, from Table 4, there can be a significant variation in the complex modulus properties depending upon the characterization method used. This fact by itself is extremely concerning to the design engineer who intends to use complex modulus data to design damped systems.

Secondly, from Figure 7, different test methods can produce different complex modulus data. The plot of loss factor versus modulus, as shown in Figure 7, is independent of frequency, temperature and α_T . The fact that there is variation between the test data in Figure 7 states simply that there are differences in the three sets of test results. These differences are generated by the inherent error in each test and the unaccounted for nonlinear frequency effect in a non-thermal-rheologically simple material.

VINAC B-100

A formulation of Vinac B-100 with a high level of mica filler was also evaluated by the BEAM, RSA II, and DMTA test methods.

Figure 13 and Figure 14 present the BEAM test results in RFN form and the inverted U plot respectively. Although there is scatter on the inverted U plot, the data appear to be reasonable representation of the complex modulus data for mica loaded B-100.

The BEAM test complex modulus data set consists of 41 complex points. A sandwich test specimen was used to generate the data. The temperature range was 72 to 270°F, while the frequency range was 240 to 4660 Hz. The WLF form of α_T with a $T_0 = 200^\circ\text{F}$ was used to generate Figure 13. It should be noted that the glassy modulus is above 10^4 psi; therefore, since the complex modulus data was collected from a sandwich test, the upper transition and glassy modulus data are inaccurate. Without the knowledge of the type or types of test specimens used, the engineer cannot judge the true accuracy of complex modulus data. Close scrutiny of the data often will not reveal inaccuracies resulting from inappropriate test specimens as can be seen in this example. This is true regardless of the test system used.

Figures 15 and 16 present the RFN and the inverted U plot for the DMTA test results of B-100. There are 160 complex data points in Figure 15 which were collected over the temperature range from 86 to 185°F and a frequency range of 0.3 to 50 Hz. A bending specimen was used during the DMTA test. The WLF form of α_T with $T_0 = 392^\circ\text{F}$ was used to generate Figure 15.

The DMTA RFN (Figure 15) contains some scatter; however, by itself, the DMTA RFN would be judged an adequate representation of the complex modulus data for B-100 with mica added.

Table 5 compares the data characterization given in Figures 13 and 15. From Table 5 one can see that the trend of the Beam T_0 being less than to DMTA T_0 continues to hold. The value of peak loss factor for the DMTA is somewhat higher than the BEAM peak value. The modulus data indicates that the rubbery data compare well but the glassy data is significantly different. As was stated earlier, the BEAM data is wrong in the glassy area.

Figure 17 presents the DMTA, BEAM, and single frequency RSA II data sets on the same RFN with $T_0 = 392^\circ\text{F}$. In this RFN comparison, the DMTA and RSA II loss factor data agree. All three data sets agree well in the transition and rubbery modulus regions; however, each set separates in the glassy region. The BEAM data has the lowest value of glassy modulus; but, as was stated earlier, the glassy data from the BEAM test is wrong because of using a sandwich test specimen to collect modulus data above 10^4 psi.

CONCLUSIONS

At the outset of this effort the intent was to discuss the limitations of and variations between three test methods for determining complex modulus properties of damping materials. However, in an effort to develop the comparison between the various test results, a variation between various α_T equations was discovered. It is quite logical to expect that some

level of variation would be generated by different α_T equations; but, it was totally unanticipated that three widely accepted α_T equations would generate such significant differences in the data.

Figure 18 presents a compilation of information on the BEAM, DMTA, and RSA II test systems. The cross-hatches area for each test system indicates modulus values where inaccurate data is often collected. In these areas the data inaccuracies may manifest themselves in a very obvious way such as negative loss factor or modulus values; or, the inaccurate data may appear to be consistent within itself such as the glassy modulus data from a sandwich beam test where the modulus values are above 10^4 psi. The accuracy, or lack thereof, in the modulus areas is dependent upon the test specimen used and the geometry of the particular test specimen. For many engineeringly practical materials, it is impossible to establish accurate complex modulus data across the entire glassy to rubbery transition with a single test specimen.

The material testers and complex modulus data users must make themselves aware of these potential problems and review not only the final complex modulus data presented but also the test procedure and test specimens used to generate the data.

The question as to which α_T relationship is the most accurate is a difficult one to answer. The S2-73 committee is working on a complex modulus data presentation standard which currently has several other α_T relationships that can be chosen besides the one used in this paper. There are many additional α_T relationships currently in use which are not considered in the S2-73 standard.

So long as engineers and scientists are also human beings, there will always be disagreement on the most appropriate test method and α_T relationship to use.

ACKNOWLEDGEMENTS

Thanks are due to Dr. D. I. G. Jones WRDC/MLLN, Dr. L. C. Rogers WRDC/FIBAA, and Mr. B. Fowler of CSA Engineering for their support in generating RFN plots for several complex modulus data sets and general discussions concerning the results.

REFERENCES

1. J. E. Ferry, Viscoelastic Properties of Polymers, John Wiley and Sons, Inc., New York, 1961.
2. D. I. G. Jones, T. Lewis, A. D. Nashif, "Frequency/Temperature Dependence of Polymer Complex Modulus Properties," Damping '89, paper number FAC.
3. L. C. Rogers, "Graphical Presentation of Damping Material Complex Modulus - Proposed Standard," ANSI (ASA)/52-73; ISO/TC108/WG13.

contrails.iit.edu

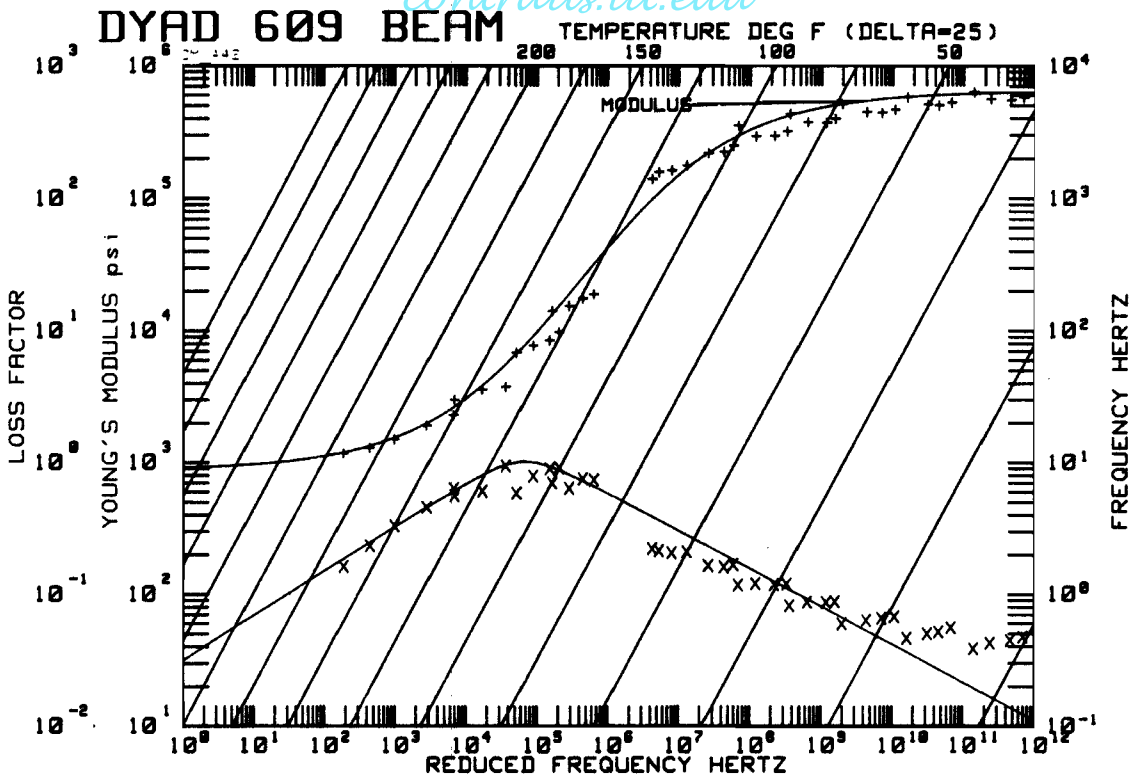


Figure 1. Dyad 609 Beam Test Results.

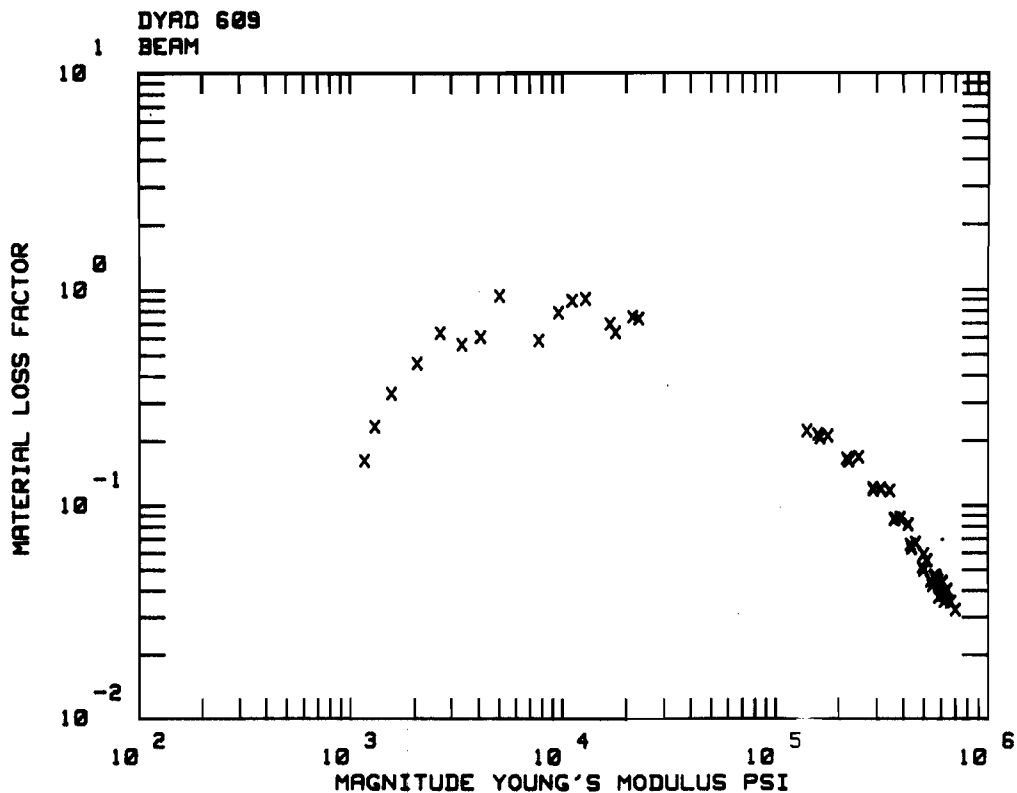


Figure 2. Dyad 609 Beam Test Complex Modulus Data.

contrails.iit.edu

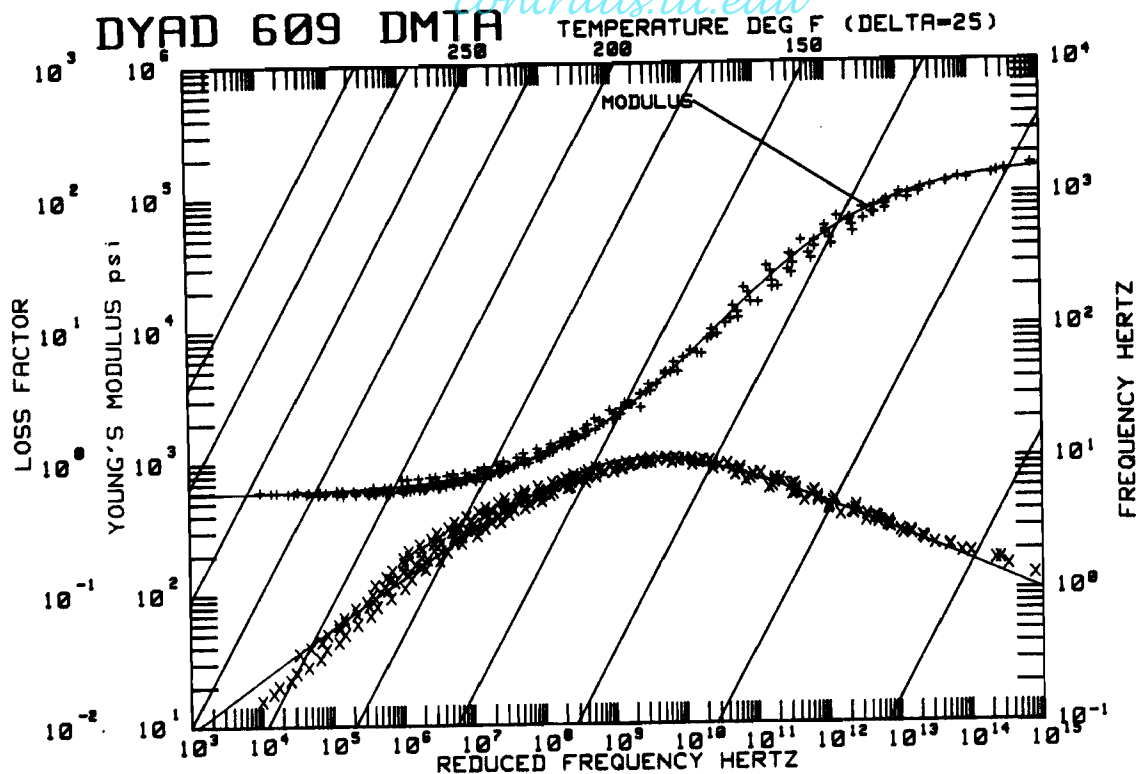


Figure 3. Dyad 609 DMTA Results.

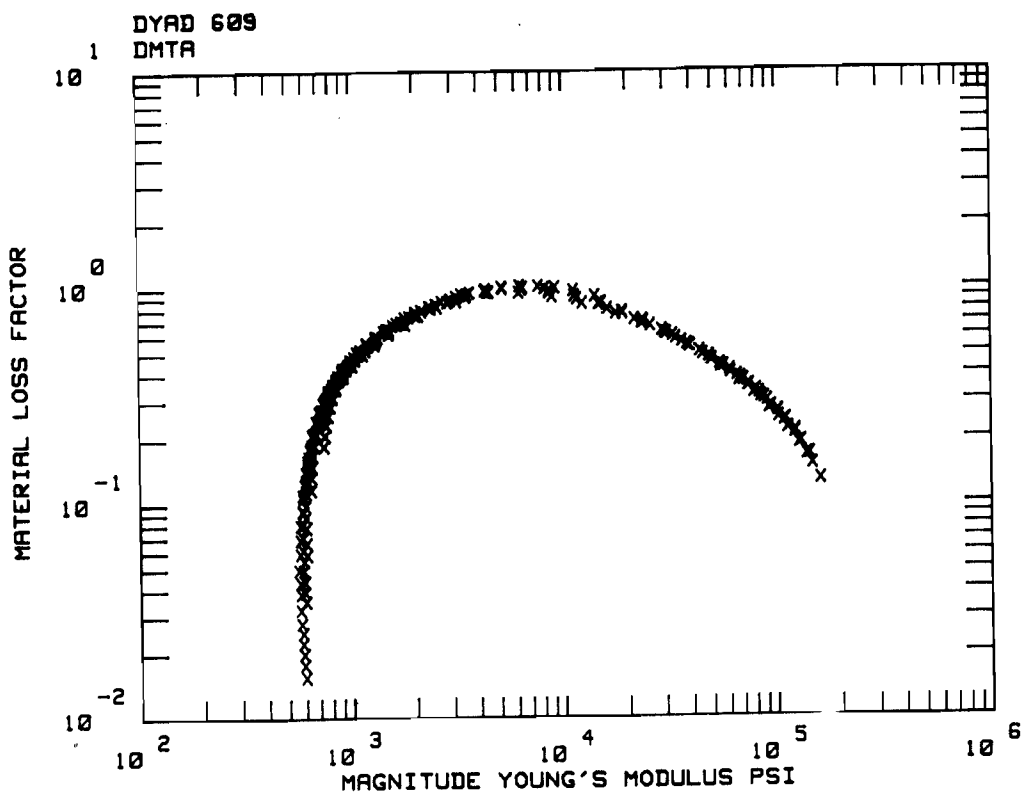


Figure 4. Dyad 609 DMTA Complex Modulus Data.

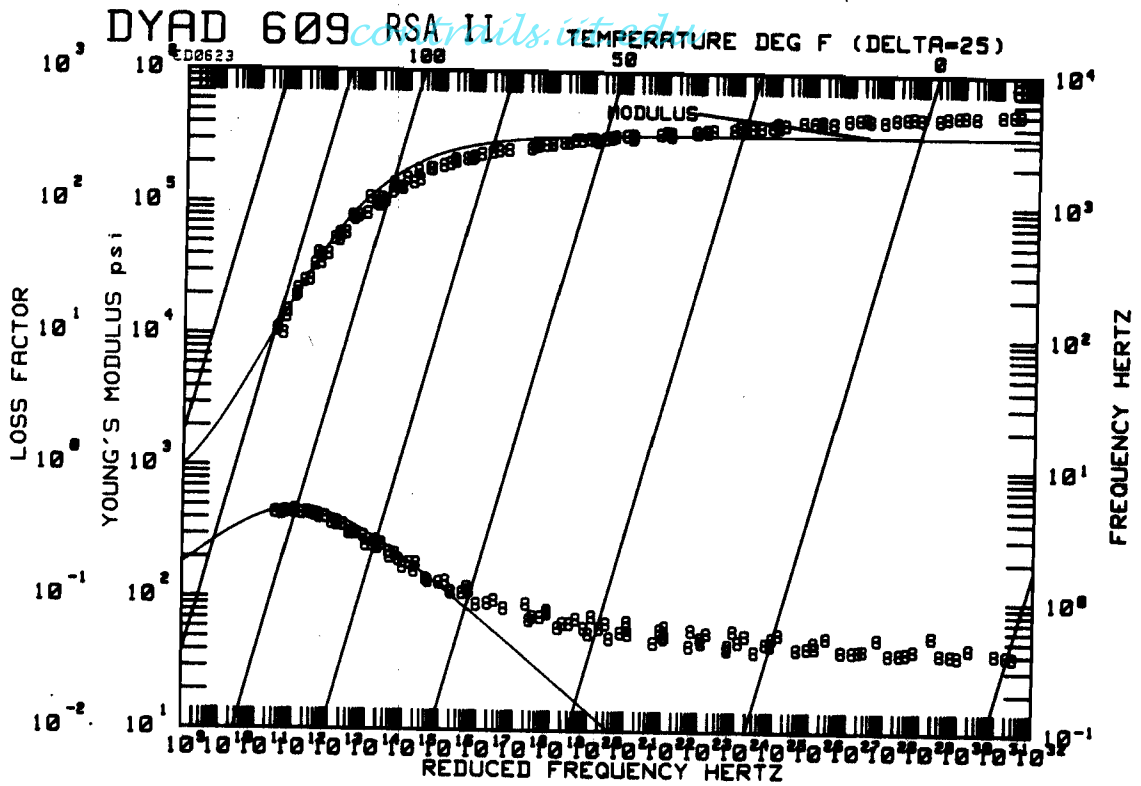


Figure 5. Dyad 609 RSA II Test Results.

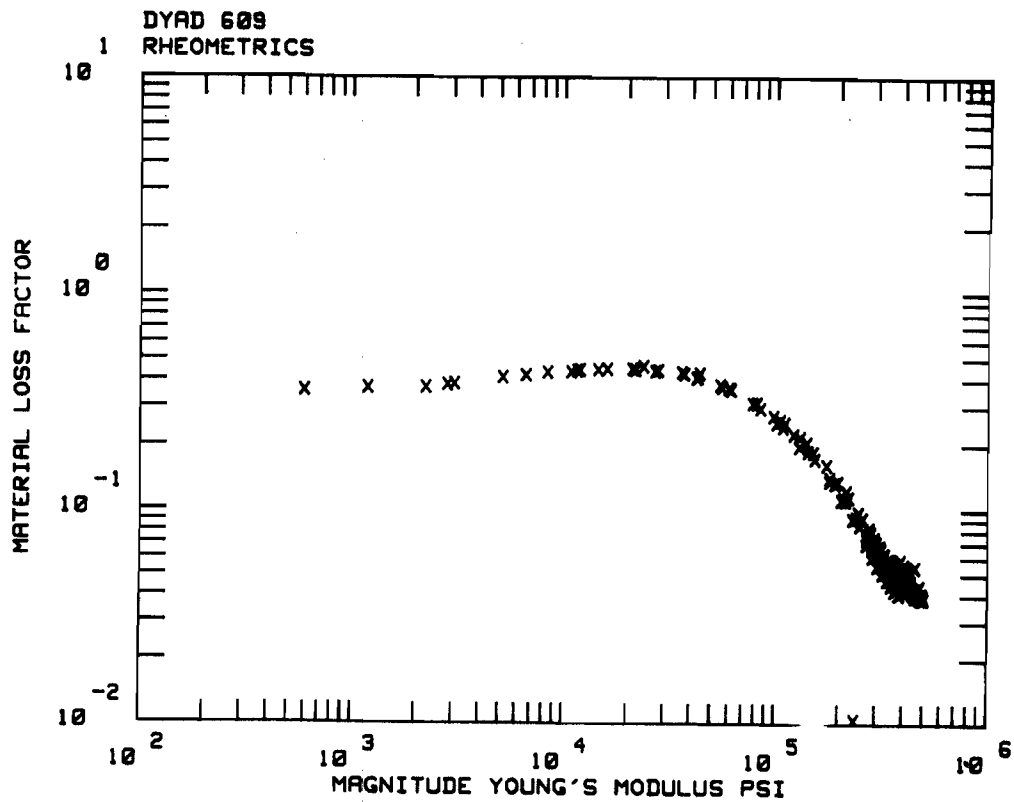


Figure 6. Dyad 609 RSA II Complex Modulus Data.

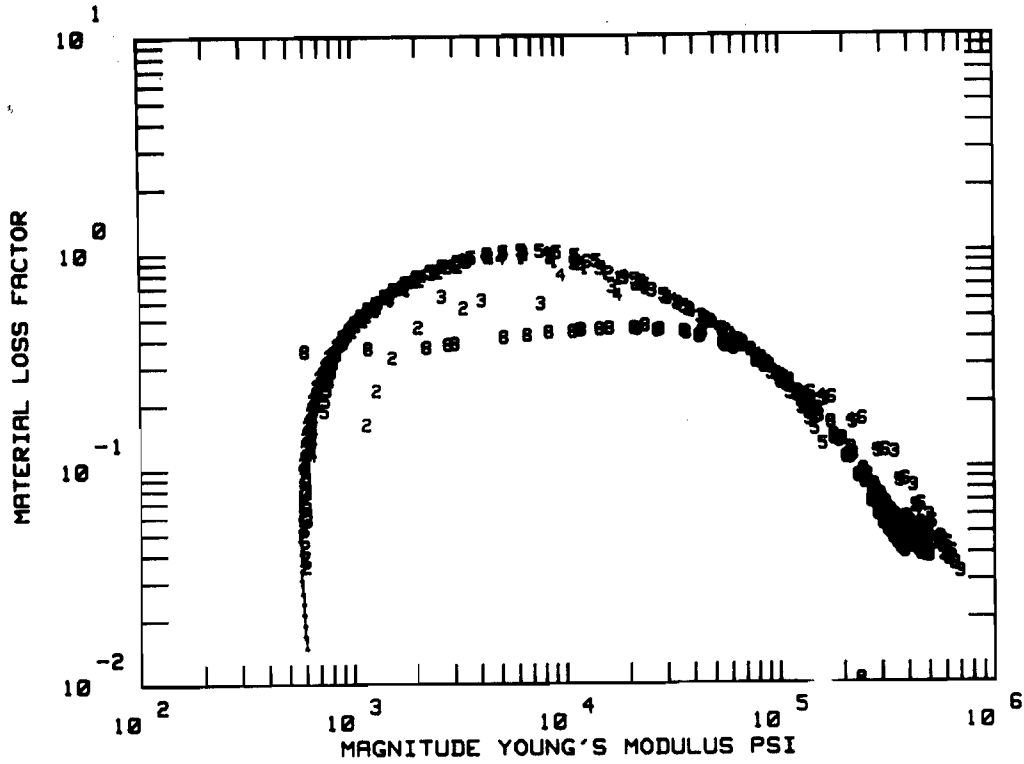


Figure 7. All 3 Complex Modulus Data Sets.

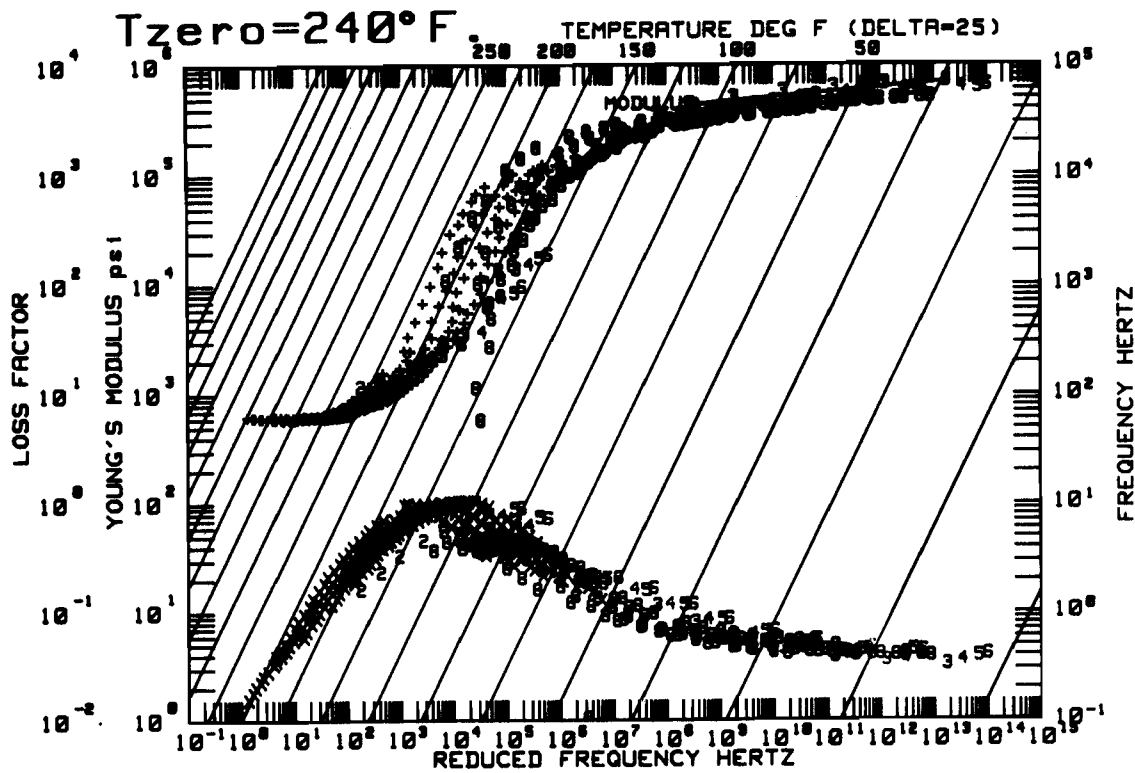


Figure 8. All 3 Complex Modulus Data Sets with $T_0 = 240^\circ\text{F}$.

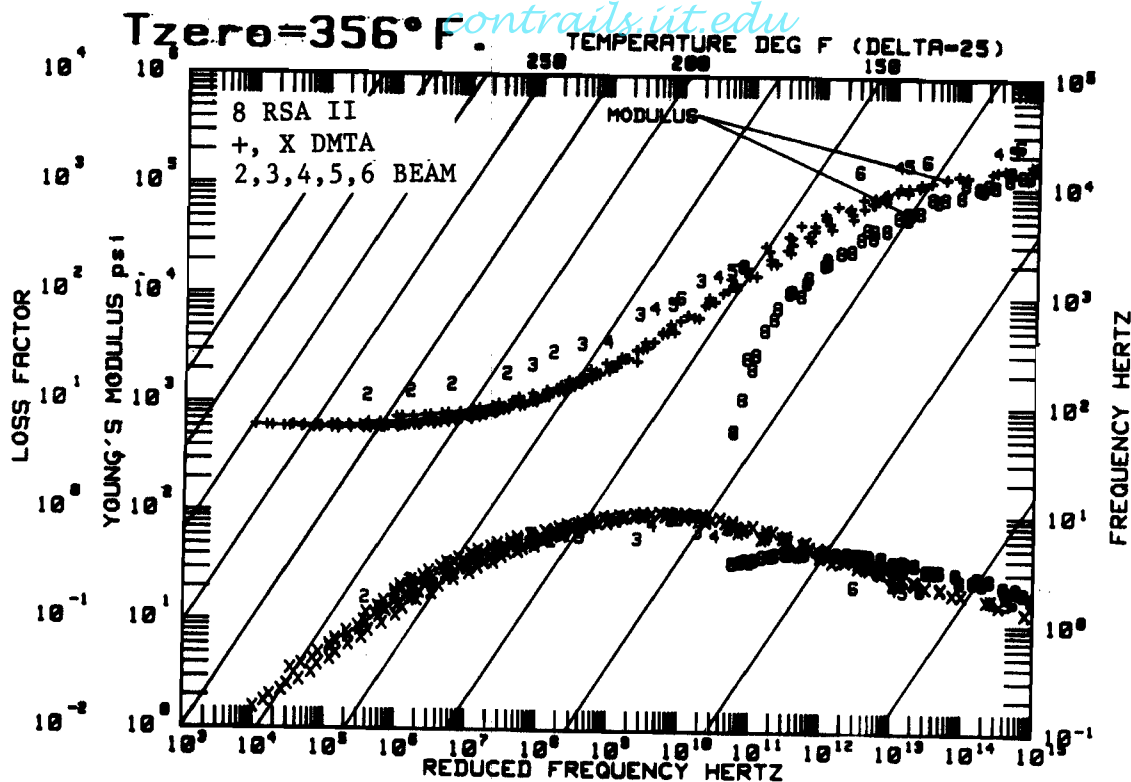


Figure 9. All 3 Complex Modulus Data Sets with $T_0 = 356^{\circ}F$.

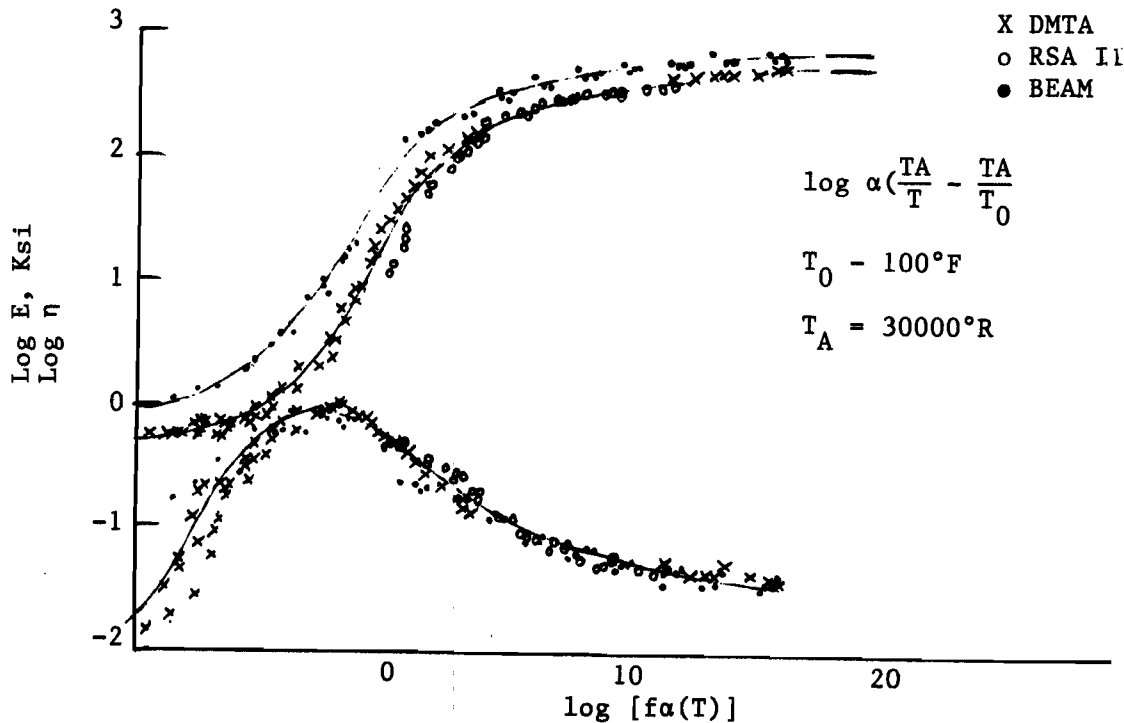


Figure 10. All 3 Data Sets Plotted with α_T Proportional to $\frac{1}{T}$.

BEAM

contrails.iit.edu

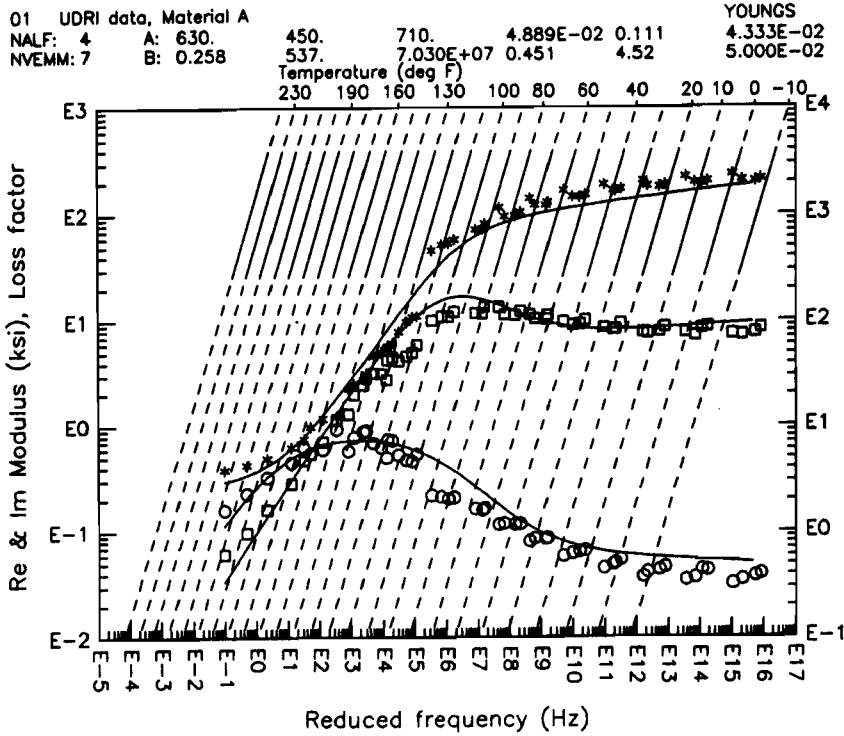


Figure 11. BEAM Data in S2-73 Draft Standard Form.

DMTA

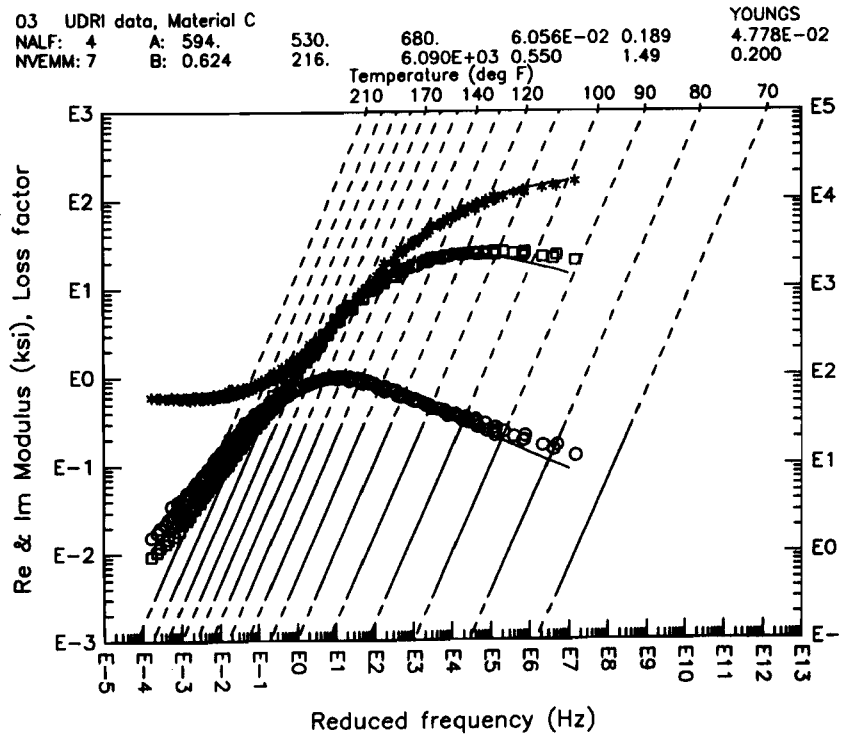


Figure 12. DMTA Data in S2-73 Draft Standard Form.

contrails.iit.edu

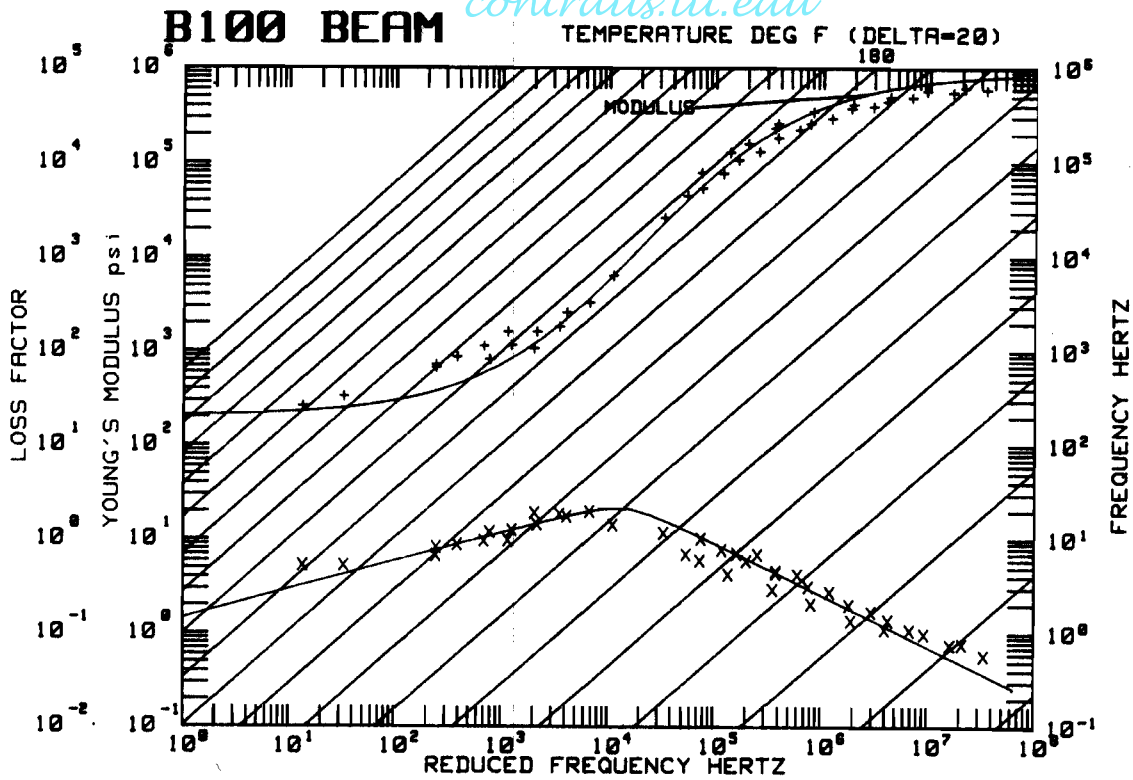


Figure 13. RFN For Vinac B-100 BEAM Test Results.

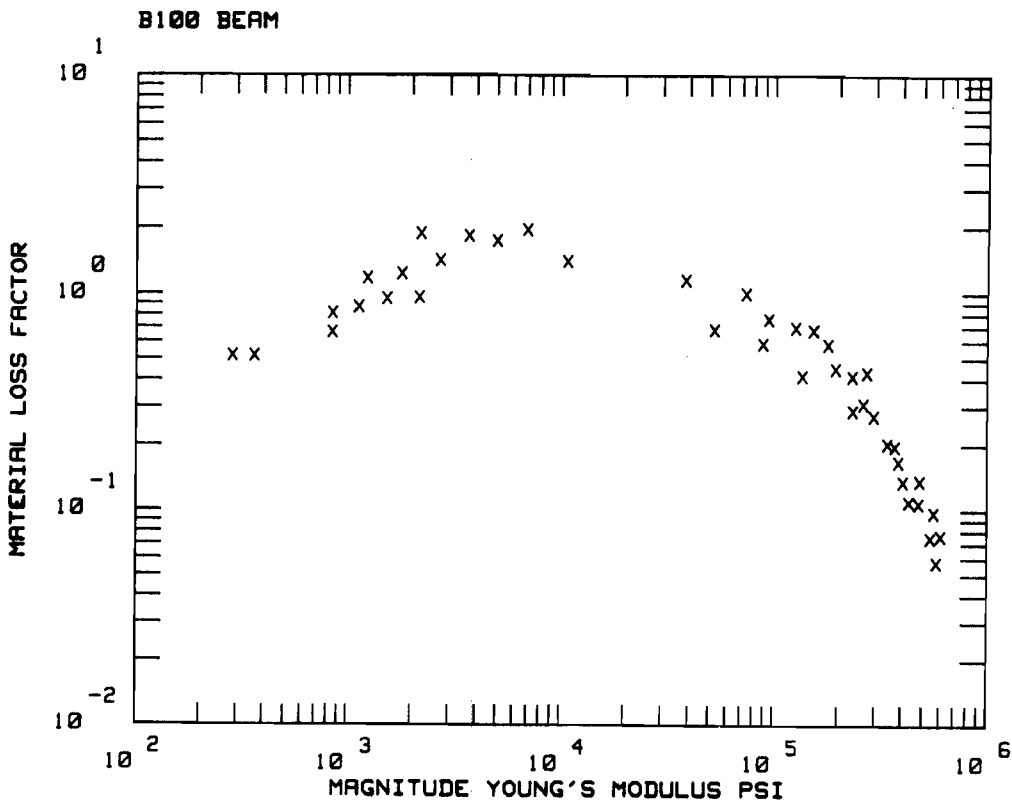


Figure 14. Complex Modulus Plot for the BEAM Test of Vinac B-100.

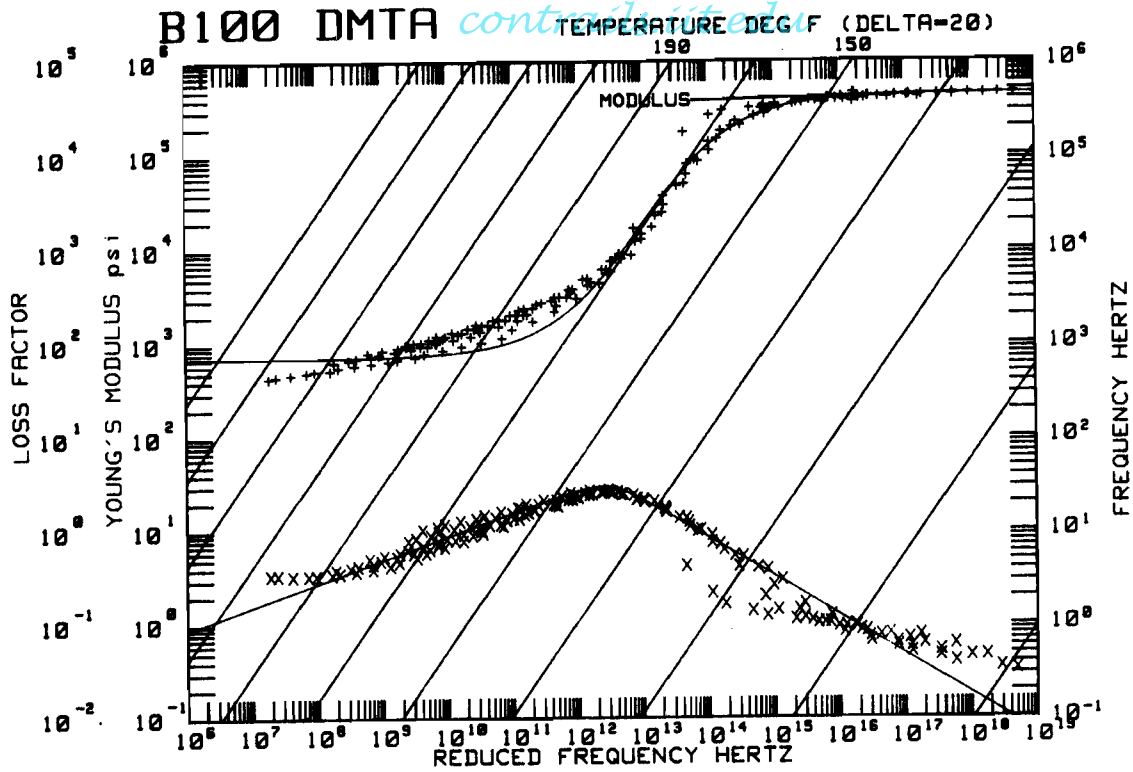


Figure 15. RFN of the DMTA Results for Vinac B-100.

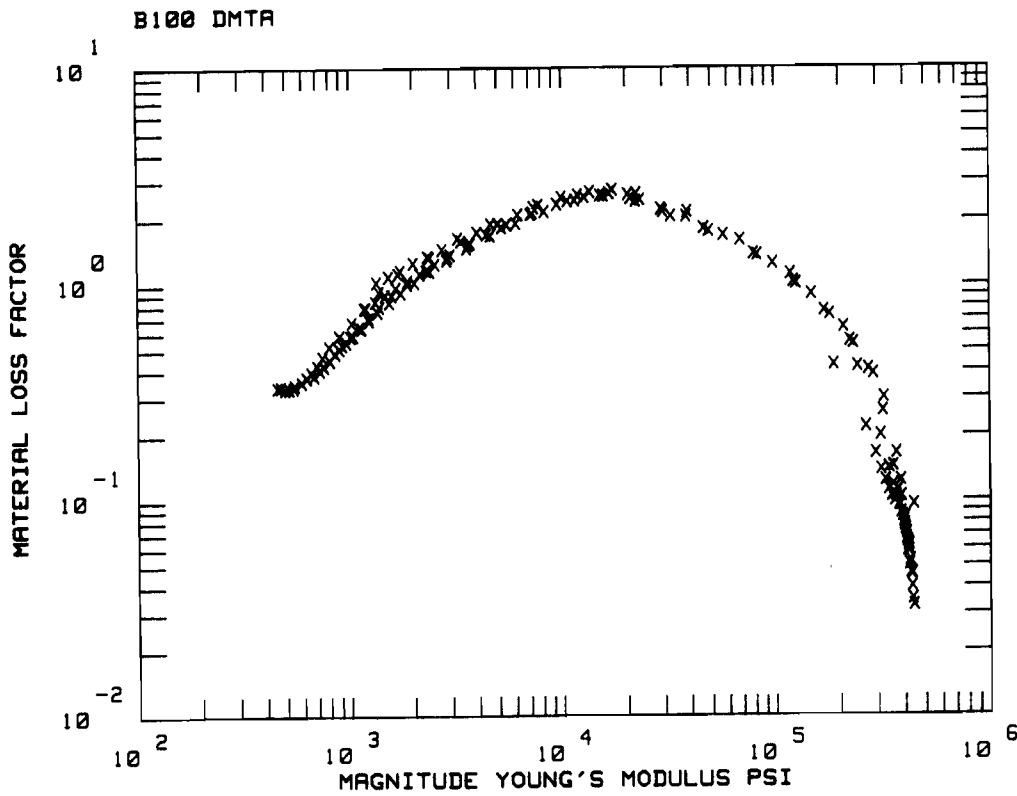


Figure 16. Complex Modulus Plot of the DMTA Results for Vinac B-100.

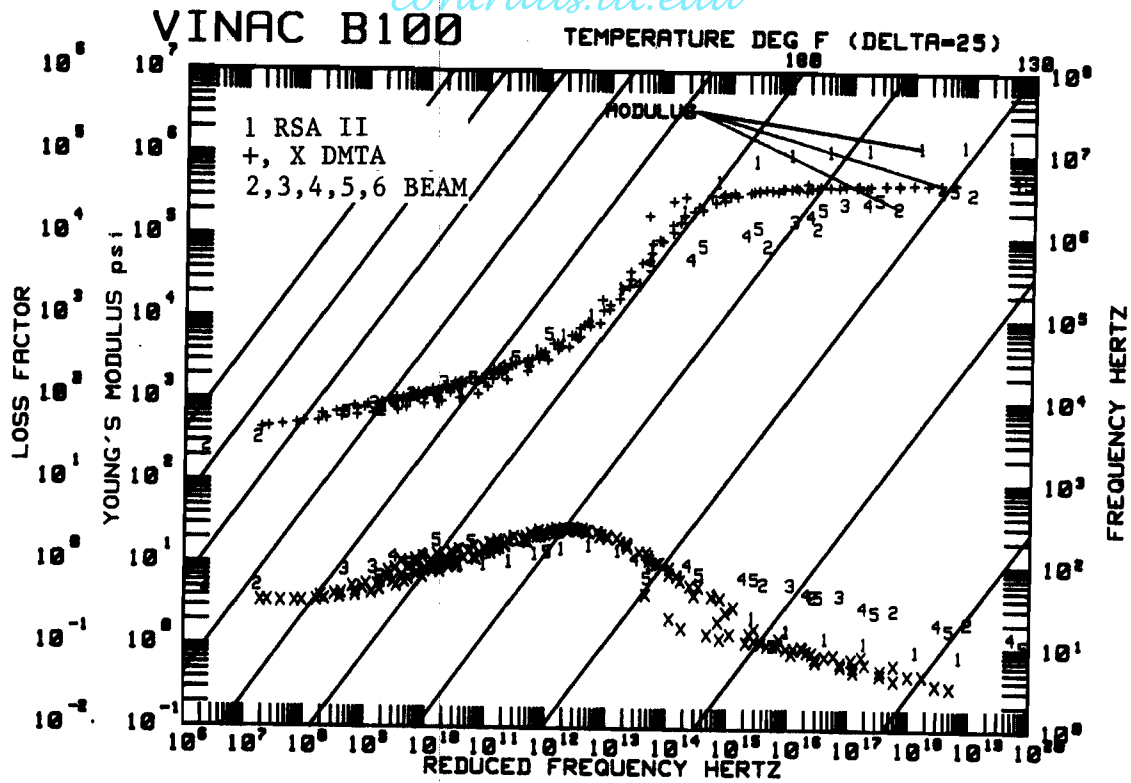


Figure 17. DMTA, BEAM, and RSA II Complex Modulus Data with $T_0 = 392$

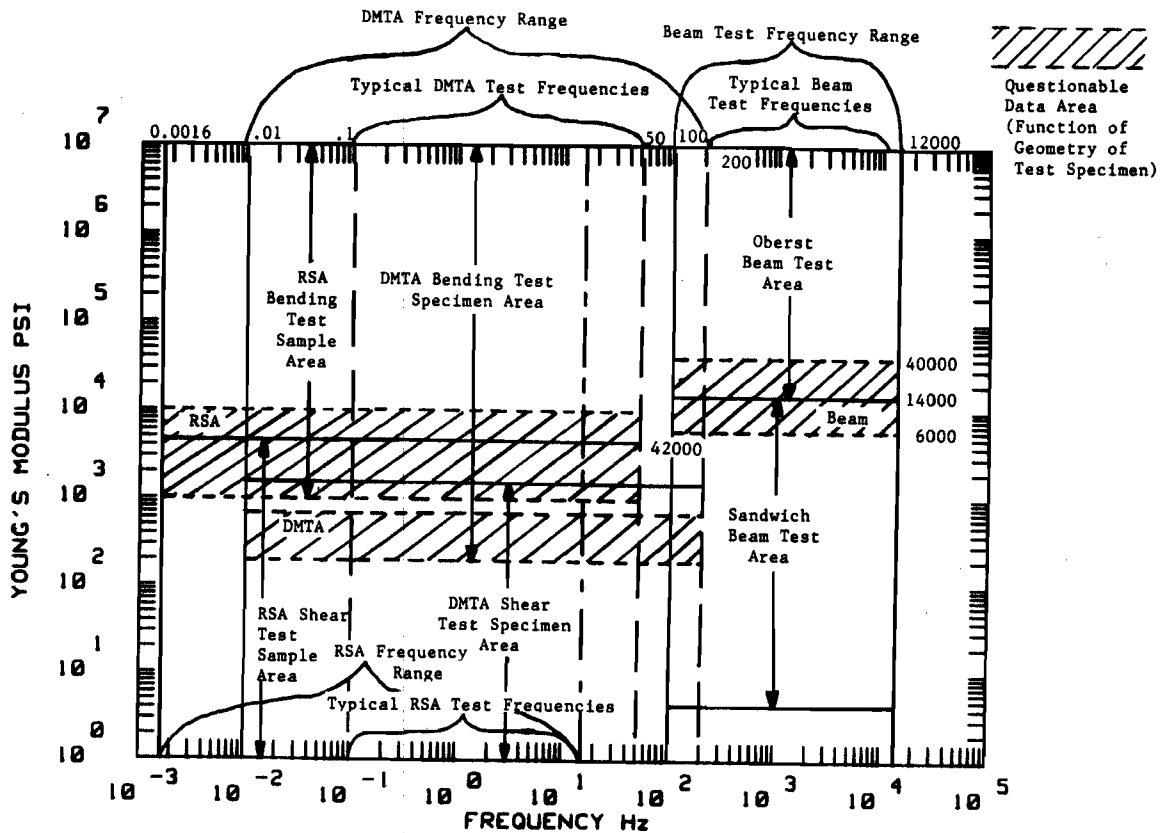


Figure 18. Frequency and Modulus Ranges Where the BEAM, DMTA, and RSA II are Usable.

TABLE 1
THE MEASUREMENT TECHNIQUES

ASTM E-756 - BEAM Test:
Frequency: 100 to 12000 Hz
Temperature: -100°F to 2000°F
Specimens: Free Layer, Sandwich, Uniform

Polymer Laboratories - DMTA:
Frequency: 0.01 to 200 Hz
Temperature: -233°F to 1472°F
Specimens: Shear & Bending

Rheometrics - RSA II:
Frequency: 0.0016 to 16 Hz
Temperature: -233°F to 1112°F
Specimens: Shear & Bending

TABLE 2
COMPARISON OF DYAD 609 CHARACTERIZATION USING THE WLF α_T

	T_0 (°F)	η_p	Modulus at η_p (PSI)	Temp. of η_p at 100 Hz (°F)	ΔT Where $\eta \geq 0.7 \eta_p$ (°F) at 100 Hz	Modulus @ 117°F and 100 Hz	Modulus @ 130°F and 100 Hz	Modulus (PSI) @ 164°F and 100 Hz	Modulus (PSI) @ 176°F and 100 Hz
BEAM	240	1.02	7742.6	140	117-164	26,266	12,703	3152.0	2319.7
DMTA	356	1.03	3396.6	154	130-176	51,418	20,237	1992.9	1273.8
RSA II*	356	N/A	N/A	N/A	N/A	N/A	N/A	N/A	N/A

* Due to the specimen used, the RSA II results did not define the peak damping level.

TABLE 3
THE S2-73 CHARACTERIZATION COMPARISON
DYAD 609

	T_0 (°F)	η_p	Modulus at η_p (PSI)	Temp. of η_p at 100 Hz (°F)	ΔT Where $\eta \geq 0.7 \eta_p$ (°F) at 100 Hz	Modulus @ 106°F and 100 Hz	Modulus @ 120°F and 100 Hz	Modulus (PSI) @ 187°F and 100 Hz	Modulus (PSI) @ 185°F and 100 Hz
BEAM	150	0.73	3569	145	106-187	27,100	11,000	656.6	700
DMTA	133	0.84	5101	154	120-185	70,000	34,406	1200.0	1350

TABLE 4
A SUMMARY OF COMPLEX MODULUS DATA CHARACTERIZATIONS EVALUATED

	Loss Factor Peak				Modulus at Peak Loss Factor (PSI)			
	WLF		$\frac{1}{T}$	$(\frac{1}{T})^2$	WLF		$\frac{1}{T}$	$(\frac{1}{T})^2$
	High T_0	Low T_0			High T_0	Low T_0		
BEAM	1.02	1.02	1.0	0.73	8200	7742	14962	3569
DMTA	1.03	1.03	1.0	0.83	5000	3346	4597	5101

TABLE 5
COMPARISON OF THE $WLF\alpha_T$ CHARACTERIZATION OF
BEAM AND DMTA COMPLEX MODULUS DATA FOR VINAC B-100

T_0 (°F)	η_p	Modulus η_p psi	Temp of η_p at 100 Hz	Modulus at 130°F & 100 Hz	Modulus at 170°F & 100 Hz	
BEAM	200	2.15	7.76E3	122	3.87E3	5.21E2
DMTA	392	3.0	4.57E3	149	1.1E5	9.5E2